RADIATION RESEARCH **156**, 365–378 (2001)
0033-7587/01 $5.00

Two-Lesion Kinetic Model of Double-Strand Break Rejoining and Cell Killing

R. D. Stewart[1]

Pacific Northwest National Laboratory, Battelle Boulevard, Richland, Washington 99352-0999

Stewart, R. D. Two-Lesion Kinetic Model of Double-Strand Break Rejoining and Cell Killing. *Radiat. Res.* 156, 365–378 (2001).

Radiobiological models, such as the lethal and potentially lethal (LPL) model and the repair-misrepair (RMR) model, have been reasonably successful at explaining the cell killing effects of radiation. However, the models have been less successful at relating cell killing to the formation, repair and misrepair of double-strand breaks (DSBs), which are widely accepted as the main type of DNA damage responsible for radiation-induced cell killing. A fully satisfactory model should be capable of predicting cell killing for a wide range of exposure conditions using a single set of model parameters. Moreover, these same parameters should give realistic estimates for the initial DSB yield, the DSB rejoining rate, and the residual number of unrepaired DSBs after all repair is complete. To better link biochemical processing of the DSB to cell killing, a two-lesion kinetic (TLK) model is proposed. In the TLK model, the family of all possible DSBs is subdivided into simple and complex DSBs, and each kind of DSB may have its own repair characteristics. A unique aspect of the TLK model is that break ends associated with both kinds of DSBs are allowed to interact in pairwise fashion to form irreversible lethal and nonlethal damages. To test the performance of the TLK model, nonlinear optimization methods are used to calibrate the model based on data for the survival of CHO cells for an extensive set of single-dose and split-dose exposure conditions. Then some of the postulated mechanisms of action are tested by comparing measured and predicted estimates of the initial DSB yield and the rate of DSB rejoining. The predictions of the TLK model for CHO cell survival and the initial DSB yield and rejoining rate are all shown to be in good agreement with the measured data. Studies suggest a yield of about 25 DSBs Gy^{-1} $cell^{-1}$. About 20 DSBs Gy^{-1} $cell^{-1}$ are rejoined quickly (15-min repair half-time), and 4 to 6 DSBs Gy^{-1} $cell^{-1}$ are rejoined very slowly (10- to 15-h repair half-time). Both the slowly and fast-rejoining DSBs make substantial contributions to the killing of CHO cells by radiation. Although the TLK model provides a much more satisfactory formalism to relate biochemical processing of DSBs to cell killing than did the earlier kinetic models, some small differences among the measured and predicted CHO cell survival and DSB rejoining data suggest that additional factors and processes not considered in the present work may affect biochemical processing of DSBs and hence cell killing. © 2001 by Radiation Research Society

INTRODUCTION

The radiobiological models that have been proposed during the last 50 years range from quasi-empirical models such as the widely used linear-quadratic (LQ) formula (*1–4*) to more mechanistic models, including the lethal and potentially lethal (LPL) model (*5*), the repair-misrepair (RMR) model (*6*), and others (*7–10*). The LPL and RMR models are representative of a class of kinetic (reaction rate) models that attempt to link radiation damage to higher-level end points through biologically plausible first- and second-order repair processes [for a review, see ref. (*11*)]. The second-order repair process is often termed binary misrepair or pairwise damage interaction. The LPL and RMR models, as well as many other models, have been reasonably successful at explaining the cell killing effects of radiation (*2, 12, 13*). However, double-strand breaks (DSBs) are widely accepted as the main type of DNA damage responsible for radiation-induced cell killing (*8–11, 14–16*), and the LPL and RMR models do not provide an entirely satisfactory formalism to directly link biochemical processing of DSBs to cell killing [e.g., see ref. (*8*)].

A fully satisfactory model should be capable of predicting cell killing for a wide range of exposure conditions using a single set of model inputs. Moreover, these same model inputs should give realistic estimates for the initial number of DSBs Gy^{-1} $cell^{-1}$, the DSB rejoining rate, and the residual number of unrepaired DSBs after all repair is complete. To improve the modeling of radiation effects for split-dose and fractionated exposure conditions, it is particularly important to model the rate of DSB rejoining accurately. Nonexponential or multiexponential DSB rejoining kinetics is often seen experimentally (*17–22*), but it is unclear whether the observed rejoining kinetics arise because radiation creates two (or possibly more) different kinds of DSBs or because of second-order repair processes such as those postulated in the LPL and RMR models. The observed DSB rejoining kinetics could also arise because repair systems saturate at higher doses or because multiple pathways and biochemical steps are involved in break-end

[1] Address for correspondence: Pacific Northwest National Laboratory, Battelle Boulevard, P.O. Box 999, MSIN K3-55, Richland, WA 99352-0999; e-mail: trebor@pnl.gov.

rejoining (*23, 24*). The experimentally observed DSB rejoining kinetics may ultimately be found to arise because multiple pathways remove a spectrum of different kinds of DSBs through first- and second-order, saturable biochemical processes.

To better link radiation damage to cell killing, this article extends and refines the formalism of the earlier LPL and RMR kinetic models to account for the possibility that radiation creates two distinct kinds of DSBs. This two-lesion kinetic (TLK) model is then used to investigate the putative link between the DSB and cell killing. As in the earlier LPL and RMR models, the TLK model includes both first- and second-order, nonsaturable repair processes. No specific assumptions are made about the biochemical steps involved in DSB rejoining. Instead, details of the DSB rejoining process are treated using the lumped parameter approach of the LPL and RMR models.

As damage repair processes are modeled in more and more detail, the number of adjustable (tunable) model parameters inevitably increases. Model calibration and testing thus becomes increasingly challenging. Goodness-of-fit statistical tests based on survival data alone (*12, 13*) are not sufficient by themselves to test postulated mechanisms of action rigorously. Consequently, the performance of the TLK model will be tested using a multi-end point approach. That is, experimental data for one biological end point (cell survival) are used to generate a model calibration. Then the performance of the model is judged by comparing measured and calibrated-model predictions for other causally related end points (number of DSBs Gy^{-1} $cell^{-1}$ and the rate of DSB rejoining). Poor agreement between the measured and model-predicted data for the test end points is an indication that the postulated mechanisms of action may be incomplete or inaccurate.

Because the TLK model is conceptually similar to earlier kinetic models, the mechanisms postulated in the TLK model are discussed and contrasted with those used in the LPL model. The performance of the TLK model is also contrasted with the performance of the LPL model. The models are calibrated using data for CHO cell survival for a rather extensive set of single-dose and split-dose exposure conditions (*25*). Large data sets such as the one reported by Stackhouse and Bedford (*25*) are needed to generate a reliable (accurate) model calibration. Then measured data for the rate of DSB rejoining in CHO cells (*26*) and the initial number of DSBs Gy^{-1} $cell^{-1}$ (*27*) are used to test the predictive power of the LPL and TLK models.

SUMMARY OF THE LPL MODEL

The original formulation of the LPL model (*5*) assumed two general classes of DNA damage: potentially lethal lesions and fatal lesions. A potentially lethal lesion is not lethal to a cell unless it interacts with another potentially lethal lesion through a pairwise (quadratic or binary misrepair) damage interaction process. Potentially lethal lesions are also removed from the DNA through biochemical processes that repair individual potentially lethal lesions without any chance the cell will be killed, i.e. a first-order (linear) repair event. That is, some potentially lethal lesions are either repaired correctly (no change in the wild-type base sequence) or they are misrepaired in a way that is not lethal to the cell (e.g., a point mutation is formed in a noncritical section of the DNA). On the other hand, a fatal lesion is an irreversible mutation or unrepairable damage that prevents a cell from ever producing viable progeny.

Curtis (*5*) tentatively suggested that potentially lethal lesions are double-strand breaks. Because DSBs are now widely believed to be the main initial type of damage responsible for cell killing, the subsequent development of the LPL model and the discussion on the mechanisms of action in the LPL model assume that potentially lethal damage is unequivocally the same as a DSB. Others have also tested the LPL model by equating the potentially lethal lesion to the DSB (*8*). In the most commonly used version of the LPL model, the DSB formation, repair and misrepair processes are modeled by a first-order, nonlinear differential equation (*5*), i.e.,

$$\frac{d\bar{L}_{dsb}(t)}{dt} = 2\dot{D}(t)Y\Sigma_{dsb} - \{\lambda_{dsb} + \eta_{dsb}\bar{L}_{dsb}(t)\}\bar{L}_{dsb}(t). \quad (1)$$

Here $\bar{L}_{dsb}(t)$ is the expected (average) number of DSBs in a cell at time t, $\dot{D}(t)$ is the instantaneous absorbed dose rate at time t (Gy h^{-1}), Y is the number of base pairs (bp) per cell, Σ_{dsb} is the expected number of DSBs initially created by radiation per nucleotide per gray (the factor of 2 converts base pairs to number of nucleotides), λ_{dsb} is the DSB repair probability (h^{-1}), and η_{dsb} is the DSB-DSB (binary misrepair) interaction probability (h^{-1}). For the special case when $\eta_{dsb} = 0$, the expected number of DSBs per cell decreases exponentially with time after irradiation. For such first-order unsaturated rejoining kinetics, it is useful to relate the repair probability λ_{dsb} to the expected DSB repair half-time τ_{dsb}, which is the expected amount of time required for a cell to remove (repair or misrepair) half of the DSBs initially produced in a cell by an acute dose of radiation. For first-order rejoining kinetics, $\lambda_{dsb} = \ln 2/\tau_{dsb}$.

The expected rate at which fatal lesions accumulate in a cell is modeled by the differential equation (*5*)

$$\frac{d\bar{L}_f(t)}{dt} = 2\dot{D}(t)Y\Sigma_f + \eta_{dsb}\bar{L}_{dsb}(t)\bar{L}_{dsb}(t), \quad (2)$$

where $\bar{L}_f$ is the expected number of fatal lesions per cell at time t and Σ_f is the expected number of fatal lesions initially created by radiation per nucleotide per gray. Equations (1) and (2) are the same as those used in the original formulation of the LPL model (*5*), but the notation is different (i.e., $2Y\Sigma_{dsb} = \eta_{PL}$, $\lambda_{dsb} = \varepsilon_{PL}$, $\eta_{dsb} = \varepsilon_{2PL}$, and $2Y\Sigma_f = \eta_L$). The LPL model has four ''adjustable'' parameters: Σ_{dsb} (or the product $2Y\Sigma_{dsb}$), Σ_f (or the product $2Y\Sigma_{dsb}$), λ_{dsb} (or equivalently τ_{dsb}), and η_{dsb}.

Interpretation of the Mechanisms of Action of the LPL Model

Ionizing radiation produces DSBs instantaneously at a rate that is proportional to the absorbed dose rate, $\dot{D}t$. First- and second-order repair processes rejoin double-strand breaks. Lethal damages are never formed by the first-order (linear) repair mechanism. On the other hand, the second-order (binary misrepair) process always produces a fatal damage. Fatal lesions are also produced directly in the DNA at a rate proportional to $\dot{D}t$. Ionizing radiation produces chromosome aberrations, and it is believed that chromosome aberrations develop from DSBs (*9, 11, 28, 29*). Thus a plausible interpretation of the mechanisms of action postulated in the LPL model is as follows:

1. Direct formation of lethal damage[2]

Curtis (*5*) suggested that the instantaneous fatal lesion production term $2Y\dot{D}(t)\Sigma_f$, arises because of intratrack proximity effects. That is, two DNA damages are formed in spatial proximity by energy deposits associated with the same particle track. Because this pairwise damage interaction process instantly converts the initial damages into an irreversible (unrepairable) form of damage, there is no chance that these lesions can undergo either a linear or a binary repair event. Because pairs of DSBs formed in this way are, by definition, never repaired, the fatal lesions arising from this process should eventually appear as simple chromosome breaks (or residual unrepaired DSBs).

An alternative explanation for the instantaneous fatal lesion production term is that some types of radiation-induced damage, perhaps a DSB accompanied by additional nearby damage, are so severe that the cell is incapable of repairing or misrepairing the initial damage. Thus a fatal lesion is created instantaneously. If this is the case, it seems likely that the direct, instantaneous formation of an unrepairable fatal lesion would again result in the eventual creation of a simple chromosome break. A third possibility is that a DSB is created in a critical gene and then rapidly misrepaired. Thus cell killing is due to the inactivation of a critical gene through mutation. However, mutations cannot be formed instantaneously. In this interpretation, the LPL mechanism of action should be viewed as an approximation to the linear misrepair mechanism included in the RMR model (*6*). A fourth possibility is that this term represents the physiochemical fixation of a DSB. The ''sticky ends'' of a DSB might interact irreversibly with histone proteins or other DNA-bound molecules to form a simple chromosome break. Or individual DSBs might be converted into unrepairable breaks or crosslinked (DNA-DNA or protein-DNA) damages by the postirradiation treatment of a cell with a chemical agent. In this interpretation, the mechanisms of action of the LPL model should again be viewed as an approximation, because the fixation process cannot occur instantaneously.

2. Binary misrepair of DSBs

The binary misrepair term $\eta_{dsb}\bar{L}_{dsb}(t)\bar{L}_{dsb}(t)$ says the rate at which break ends associated with two different DSBs are incorrectly rejoined is proportional to the square of the number of unrepaired DSBs in a cell. The expected number of break ends in a cell at time t is $2\bar{L}_{dsb}(t)$. The incorrect rejoining of break ends associated with two different DSBs involves relatively large sections of DNA, and misrepaired damages formed by the binary misrepair mechanism are reasonably linked to various classes of intra- or interchromosomal (complete or incomplete exchange-type) aberrations, e.g. dicentrics, acentric rings, and translocation aberrations. When the pairwise damage interaction process is complete, an acentric fragment will be formed along with the dicentric or acentric ring. If the DSB interaction process is incomplete, the dicentric or acentric ring will be accompanied by two acentric chromosome fragments. One of the two is an excess acentric fragment.

As a model to predict the yields of chromosome aberrations, the LPL model has some obvious limitations. On theoretical grounds, Sachs *et al.* (*11*) have suggested that the binary misrepair term in Eq. (2) should be multiplied by a factor of 1/4 to account for the creation of nonlethal chromosome aberrations (e.g. translocations) and for the fact that two DSBs disappear each time one dicentric or centric ring plus an accompanying acentric fragment is formed. Also, the complex aberrations (*30*) formed at higher doses through the rejoining of break ends associated with more than two DSBs are not explicitly modeled. However, the LPL model is capable of predicting the cell killing effects accurately, even for doses as high as 25 to 50 Gy [e.g., see ref. (*5*)]. This observation suggests that complex aberrations may be formed through the sequential or simultaneous rejoining of multiple break-end pairs. That is, multiple DSBs are required to form a complex aberration, but the rate at which break ends are misjoined is still proportional to $\bar{L}_{dsb}(t)\bar{L}_{dsb}(t)$.

Within the framework of the LPL model, the fatal lesions responsible for cell killing are reasonably interpreted as a mix of dicentrics, acentric rings, chromosome breaks, and, for large doses, complex aberrations formed through the rejoining of break ends associated with multiple DSBs. For dose conditions in which many complex aberrations are formed, the outputs of the LPL model cannot be compared easily to measured yields of aberrations. However, for lower-dose conditions, comparisons of the outputs of the LPL model and some types of aberration yields may be reason-

[2] As a phenomenological model to predict cell killing, the fine points of the interpretation of the direct fatal lesion production term are moot. However, for the purposes of testing postulated mechanisms of action, they may not be moot. If the direct fatal lesion production term represents a kinetic process such as physiochemical fixation or damage misrepair, it may be possible to alter the fate of the damage by manipulating the cell microenvironment after irradiation. On the other hand, if the process is instantaneous and irreversible, postirradiation manipulation of the cellular environment should not affect the fate of the damage.

able. Each acentric fragment plus an acentric ring or dicentric should be counted as a single fatal lesion (*11*). Extra (residual or nonpaired) chromosome breaks should also be counted as fatal lesions. In the LPL model, these residual chromosome breaks are accounted for in the direct fatal lesion production term, $2\dot{D}(t)Y\Sigma_f$. The fractional number of unrepaired (residual) DSBs measured using techniques such as PFGE should be approximately equal to $\Sigma_f/(\Sigma_{dsb} + \Sigma_f)$.

THE TWO-LESION KINETIC MODEL

As in the LPL model, ionizing radiation produces DSBs instantaneously at a rate that is proportional to the absorbed dose rate $\dot{D}(t)$, and first- and second-order repair processes rejoin the DSB break ends. However, in the TLK model, the family of all possible DSB configurations is subdivided into simple and complex DSB types, and each kind of DSB may have unique damage repair characteristics. As a working hypothesis, a simple DSB is assumed to be a section of the DNA 10 to 20 bp in length that contains a break in each strand of the DNA. A complex DSB is a simple DSB that contains additional elementary damage sites (base damage, strand breaks, base deletion, etc.) within the same section of DNA. Another difference is that the TLK model replaces the direct fatal lesion production term that is included in the LPL model with a physiochemical (not related to repair) damage fixation mechanism and includes terms to account for the linear misrepair of DSBs, as postulated in the RMR model (*6*). Chromatin-related effects (*31–35*) are treated implicitly in the TLK model using a single chromatin domain or state.

Double-strand break formation, repair and misrepair processes are modeled by two first-order, nonlinear differential equations in the TLK model; i.e.,

$$\frac{d\bar{L}_1(t)}{dt} = 2\dot{D}(t)Y\Sigma_1 - \{\varepsilon_1 + \lambda_1\}\bar{L}_1(t) - \bar{L}_1(t)[\eta_1\bar{L}_1(t) + \eta_{1,2}\bar{L}_2(t)] \quad (3)$$

$$\frac{d\bar{L}_2(t)}{dt} = 2\dot{D}(t)Y\Sigma_2 - \{\varepsilon_2 + \lambda_2\}\bar{L}_2(t) - \bar{L}_2(t)[\eta_{1,2}\bar{L}_1(t) + \eta_2\bar{L}_2(t)]. \quad (4)$$

Here $\bar{L}_1(t)$ is the expected number of simple (Type I) DSBs per cell at time t, and $\bar{L}_2(t)$ is the expected number of complex (Type II) DSBs per cell at time t. The DSB parameters Σ_1, Σ_2, λ_1, λ_2, η_1, η_2 and $\eta_{1,2}$ have a biophysical interpretation analogous to the λ_{dsb} and η_{dsb} parameters used in the LPL model. The parameters ε_1 and ε_2 account for physiochemical fixation of DSBs.

The misrepair of a DSB results in either a lethal or a nonlethal genetic alteration in the DNA. However, in the TLK model, fixation always produces a lethal DNA damage. The time-dependent accumulation of lethal DNA damage in a cell is modeled by

$$\frac{d\bar{L}_f(t)}{dt} = [(1 - a_1)\beta_1\lambda_1 + \varepsilon_1]\bar{L}_1(t) + [(1 - a_2)\beta_2\lambda_2 + \varepsilon_2]\bar{L}_2(t) + \gamma_1\eta_1\bar{L}_1(t)\bar{L}_1(t) + 2\gamma_{1,2}\eta_{1,2}\bar{L}_1(t)\bar{L}_2(t) + \gamma_2\eta_2\bar{L}_2(t)\bar{L}_2(t), \quad (5)$$

where a_1 and a_2 represent the fidelity of the linear misrepair mechanism (e.g., $a_1 = a_2 = 1$ indicates correct repair). The probabilities β_1, β_2, γ_1, $\gamma_{1,2}$ and γ_2 partition misrepaired damages into lethal and nonlethal genetic alterations. For example, $\beta_1 = 1$ means that linear misrepair of the first kind of DSB always produces a fatal lesion. The yield of nonlethal genetic alterations (i.e. mutations) produced in a cell can be plausibly linked to the activation or inactivation of critical genes, the induction of genome instability, and neoplastic transformation (*36–38*). The equation describing the accumulation of nonlethal mutations is

$$\frac{d\bar{L}_m(t)}{dt} = (1-a_1)(1-\beta_1)\lambda_1\bar{L}_1(t) + (1-a_2)(1-\beta_2)\lambda_2\bar{L}_2(t) + (1 - \gamma_1)\eta_1\bar{L}_1(t)\bar{L}_1(t) + (1 - \gamma_2)\eta_2\bar{L}_2(t)\bar{L}_2(t) + 2(1 - \gamma_{1,2})\eta_{1,2}\bar{L}_1(t)\bar{L}_2(t). \quad (6)$$

Interpretation of the Mechanisms of Action of the TLK Model

In both the LPL and TLK models, the fatal lesions responsible for cell killing are mainly dicentrics, acentric rings, chromosome breaks, and, for large doses, complex aberrations formed through the rejoining of break ends associated with multiple DSBs. Binary misrepair of DSB break ends produces exchange-type chromosome aberrations (dicentrics, acentric rings, and translocations). A unique feature of the TLK model is that break ends associated with both simple and complex DSBs can interact in pairwise fashion to form an exchange-type aberration. The TLK model, unlike the LPL model, also includes damage fixation and linear misrepair mechanisms. The interpretation of these mechanisms is as follows:

1. Linear misrepair

The linear misrepair mechanisms, $(1 - a_1)\lambda_1\bar{L}_1(t)$ and $(1 - a_2)\lambda_2\bar{L}_2(t)$, describe the incorrect rejoining of break ends associated with individual DSBs. Since the linear misrepair of individual DSBs most likely involves relatively small sections of damaged DNA (~1 to 10 bp), this DSB mechanism is most likely to produce either a point mutation or a deletion-type aberration. If multiple strand breaks and other elementary damage sites are located within a few base pairs of each other, it seems likely that the probability of correct repair (a_1 and a_2) is zero. The probability of correct repair may even be close to zero for simple DSBs. How-

ever, because most randomly formed point mutations and deletion-type aberrations will not affect the control or coding section of a critical gene, the probability of lethal misrepair (β_1 and β_2) is most likely small. Based on the amount of DNA associated with critical ''housekeeping'' genes, values of β_1 and β_2 of the order of 0.1% to 10% are expected for a typical mammalian cell.

2. Damage fixation

The damage fixation mechanisms, $\varepsilon_1\bar{L}_1(t)$ and $\varepsilon_2\bar{L}_2(t)$, describe the time-dependent conversion of DSBs into lethal damages by processes that are not related to biochemical repair (i.e., the physiochemical fixation process discussed in the Summary of the LPL Model). Because the fixation and linear misrepair of damages occurs at a rate that is proportional to the number of DSBs in a cell [i.e., $\bar{L}_1(t)$ and $\bar{L}_2(t)$], it may be difficult to distinguish the linear misrepair mechanism from the fixation mechanism if only data on cell killing are used to test the model. However, in principle, damage fixation can be differentiated from linear misrepair of a DSB, because the fixation mechanism produces chromosome breaks (residual unrepaired DSBs) while the linear misrepair mechanism produces point mutations or deletion-type aberrations. Alternatively, a mutation that inactivates a key repair gene will most likely alter the DSB rejoining parameters (λ_1, λ_2, η_1, $\eta_{1,2}$ and η_2) but not the DSB fixation parameters ε_1 and ε_2.

METHODS

Numerical Solution of the LPL and TLK Models

As a guide to the development of more realistic models for damage repair processes, Stewart, Shultis and Montelone developed a very general multilesion, multistate (MLMS) kinetic model (*39*). The formalism of the MLMS model is sufficiently general to account for differences in the initial DNA damage yield among chromatin types (e.g. euchromatin and heterochromatin), and it allows for the inclusion and tracking of an arbitrary number of different types of lethal and nonlethal damages. The general MLMS model has been implemented in the Kinetic Biological Effects Modeling (KBEM) software package.[3] Because the LPL, RMR and TLK models are all special cases of the general kinetic model (*39*), the KBEM software can be used to simulate radiobiological effects using any one of these models.

The KBEM software uses Visual Numeric's (http://www.vni.com) IMSL® DIVPAG routine to integrate the MLMS system of differential equations forward in time using Gear's backward differentiation algorithm (*40, 41*) for an arbitrarily complex dose-rate function $\dot{D}(t)$. Analytical and numerical (KBEM-based) solutions for the LPL and RMR models agree to better than six significant digits for a wide range of absorbed dose and dose-rate exposure conditions. Additional testing indicates that the KBEM software solves the system of differential equations used in the TLK model to the same level of accuracy.

Calculation of Cell Survival Probabilities

In delayed-plating experiments, the metabolic status of a cell is modified at some specific time after irradiation. For example, cells are shifted from conditioned medium to growth medium several hours after irradiation. Cells are shifted to a growth medium so that the reproductive viability of the cells can be tested. Alternatively, confluent, density-inhibited cells are irradiated and then incubated under the same conditions for several hours before they are placed in growth medium. Changing the metabolic status of a cell introduces a fundamental discontinuity into the modeling of damage repair processes. That is, the kinetics of damage repair before and after plating is likely quite different.

A common way to approach the analysis of delayed-plating experiments is to assume that all the unrepaired damage in a cell becomes irreversible and lethal at some fixed (effective) time after irradiation (*5, 8*). In general, it is not correct to assume that the time available for repair is always the same as the interval before the cells are plated (*8*); i.e., unrepaired DSBs are not necessarily converted into irreversible and lethal DNA damage the instant the cells are placed in growth medium.

The LPL and TLK models can be used to provide estimates of the expected amount of lethal DNA damage in a cell as a function of time during and after irradiation. The differential equations describing the formation, repair and misrepair of DNA damage [Eqs. (1) and (2) for the LPL model or Eqs. (3) to (6) for the TLK model] are integrated forward in time until a cutoff time is reached (the effective time available for repair) or until all of the radiation damage is repaired correctly, rejoined incorrectly, or fixed (i.e., the time available for repair is effectively infinite). If the cutoff time is reached before all of the damage is repaired, misrepaired or fixed, it is assumed that the damage becomes irreversible and lethal. Prior to irradiation, it is assumed that no DSBs or fatal lesions are present, so that $\bar{L}_{dsb}(0) = \bar{L}_f(0) = 0$ (LPL model) or $\bar{L}_1(0) = \bar{L}_2(0) = \bar{L}_f(0) = 0$ (TLK model). The expected fraction of cells surviving irradiation is $S = \exp\{-\bar{L}_f\}$ (*5, 11*). Here $\bar{L}_f$ denotes the expected number of fatal lesions per cell at the end of the simulation (i.e., after the time cutoff is reached or all of the initial damage is repaired, misrepaired or fixed).

In general, $\bar{L}_f(t)$ for $t > t_0$ approaches the value $\bar{L}_f(\infty)$ at an exponential rate. Here t_0 is the time when the radiation exposure ends. For $t > t_0 + n/\lambda_{dsb}$ (LPL model) or $t > t_0 + n/\min(\lambda_1,\lambda_2)$ (TLK model), $\bar{L}_f(t)$ is indistinguishable from $\bar{L}_f(\infty)$ for values of n greater than about 10 or 15, that is, for times equivalent to 10 or 15 DSB repair half-times after the irradiation ends. Even for $n \gtrsim 2$, a large fraction of the initial DSBs will already be repaired correctly, misjoined or fixed, so that it may be challenging to detect changes in cell survival for delayed plating times greater than about 2 or 3 DSB repair half-times. Except where explicitly noted otherwise, it is assumed in this article that the time available for repair is effectively infinite.

Calculation of the Fraction of the Activity Released (FAR) out of the Well

Data on the rate of DSB rejoining are often reported in the earlier literature in terms of FAR (percentage DNA released from the plug). The random breakage model (*42, 43*) provides a suitable formalism to convert the predictions of the model for the number of unrejoined DSBs into an estimate of FAR. The equation converting unrepaired DSBs into FAR is (*44*)

$$\mathrm{FAR} = F_{max}\left\{1 - \left[1 + K\bar{N}_{dsb}\left(1 - \frac{K}{M_0}\right)\right]\exp^{-K\bar{N}_{dsb}}\right\}. \qquad (7)$$

Here F_{max} is the maximum fraction of the cellular DNA that can enter the gel, M_0 is the average chromosome size, and K is the gel exclusion size (DNA fragments larger than K do not move out of the well). At various times after the irradiation ends, $\bar{N}_{dsb}$ is set equal either to $\bar{L}_{dsb}(t)/Y$ (LPL model) or to $[\bar{L}_1(t) + \bar{L}_2(t)]/Y$ (TLK model). In general, the fraction of the DNA migrating out of the agarose plug (well) tends to increase as the gel exclusion size increases and decreases as the average chromosome size increases.

Stackhouse and Bedford (*26*) collected data on DSB rejoining for quiescent CHO cells using electrophoresis conditions that separated either *Saccharomyces cerevisiae* chromosomes (260–2500 kbp) or *Schizosaccaromyces pombe* chromosomes (3–7 Mbp). A gel exclusion-size parameter in the range from 2 Mbp to 8 Mbp is appropriate for this data set.

[3] See http://www.pnl.gov/berc/kbem/.

Except where explicitly stated otherwise, the results reported in this article are based on $F_{max} = 1$, $Y = 4682 \times 10^6$ bp (*45*), $K = 6 \times 10^6$ bp, and $M_0 = 101.8 \times 10^6$ bp (~46 chromosomes/cell).

Lower and Upper Bounds on LPL Parameters

Although the DSB yield $2Y\Sigma_{dsb}$ (Gy^{-1} $cell^{-1}$) and the repair probability λ_{dsb} (h^{-1}) can be measured or at least constrained to a reasonable range of values, computer-based techniques to automatically optimize or ''tune'' these parameters as well as identify values for the misrepair probability η_{dsb} (h^{-1}) and fatal lesion yield $2Y\Sigma_f$ (Gy^{-1} $cell^{-1}$) are of obvious practical value. Because constrained parameter optimization tasks are often easier than unconstrained ones, it is useful to establish bounds on all model inputs. All four of the input parameters used in the LPL model can be constrained to non-negative values on biophysical grounds. Further, the initial DSB yield is about 23 to 28 Gy^{-1} $cell^{-1}$ for Chinese hamster cells (*27*),[4] and the repair probability λ_{dsb} can be conservatively constrained to values between 0.0277 h^{-1} (25-h repair half-time) to 20.79 h^{-1} (2-min repair half-time) (*22*).

An upper bound on the yield of fatal lesions can be established by solving Eq. (2) for the special case when $\eta_{dsb} = 0$. Namely, for an absorbed dose $D > 0$,

$$2Y\Sigma_f \leq -\frac{\ln S(D)}{D}, \tag{8}$$

where $S(D)$ is a measured cell survival probability for some exposure condition. Because of the interplay between DSB formation, repair and binary misrepair processes, and uncertainties in the input parameters associated with these processes, a simple analytical expression that establishes a firm upper limit on the binary misrepair interaction probability is not possible. However, for a given level of radiation-induced cell killing, the value of η_{dsb} must, in general, decrease as the value of $2Y\Sigma_{dsb}$ increases and increase as the value of λ_{dsb} increases.

Lower and Upper Bounds on the Parameters of the TLK Model

The most general form of the TLK model has 16 biologically significant parameters (a_1, β_1, γ_1, Σ_1, λ_1, η_1, ε_1, a_2, β_2, $\eta_{1,2}$, $\gamma_{1,2}$, γ_2, Σ_2, λ_2, η_2 and ε_2). On biophysical grounds, the following constraints can be imposed with no loss in the generality of the model.

$$0 \leq a_1, \beta_1, a_2, \beta_2, \gamma_1, \gamma_{1,2}, \gamma_2 \leq 1, \tag{9}$$

$$0 \leq \lambda_1, \varepsilon_1, \lambda_2, \varepsilon_2, \eta_1, \eta_{1,2}, \eta_2, \tag{10}$$

$$0 \leq \Sigma_1, \Sigma_2. \tag{11}$$

To reduce the number of adjustable parameters, the following additional (*ad hoc*) equality constraints are imposed in this work: $a_1 = a_2 = 0$ (repair of a DSB always results in a lethal or nonlethal mutation), $\varepsilon_1 = \varepsilon_2 = 0$ (no DSB fixation), $\gamma_1 = \gamma_{1,2} = \gamma_2 = \gamma$, and $\eta_1 = \eta_{1,2} = \eta_2 = \eta$. Under these constraints, Eqs. (3), (4), (5) and (6) simplify to

$$\frac{d\bar{L}_1(t)}{dt} = 2\dot{D}(t)Y\Sigma_1 - \lambda_1\bar{L}_1(t) - \eta\bar{L}_1(t)[\bar{L}_1(t) + \bar{L}_2(t)], \tag{12}$$

$$\frac{d\bar{L}_2(t)}{dt} = 2\dot{D}(t)Y\Sigma_2 - \lambda_2\bar{L}_2(t) - \eta\bar{L}_2(t)[\bar{L}_1(t) + \bar{L}_2(t)], \tag{13}$$

$$\frac{d\bar{L}_f(t)}{dt} = \beta_1\lambda_1\bar{L}_1(t) + \beta_2\lambda_2\bar{L}_2(t) + \gamma\eta[\bar{L}_1(t) + \bar{L}_2(t)]^2, \tag{14}$$

$$\frac{d\bar{L}_m(t)}{dt} = (1 - \beta_1)\lambda_1\bar{L}_1(t) + (1 - \beta_2)\lambda_2\bar{L}_2(t) + (1 - \gamma)\eta[\bar{L}_1(t) + \bar{L}_2(t)]^2. \tag{15}$$

For Chinese hamster cells, the quantity $2Y(\Sigma_1 + \Sigma_2)$ equals about 25 DSBs Gy^{-1} $cell^{-1}$. The repair probabilities λ_1 and λ_2 can be constrained to the range 0.0277 h^{-1} (25-h repair half-time) to 20.79 h^{-1} (2-min repair half-time). Numerical studies using representative parameters for the TLK model suggest that the binary misrepair probability, η, is most likely less than 10^{-3} to 10^{-2} h^{-1}.

Automated Identification of Model Inputs

The main goal of model optimization (calibration) is to identify the set of model inputs that gives the best possible agreement between model-predicted quantities and experimental observations. To accomplish this goal, standard model calibration techniques typically seek to identify an optimal parameter set by minimizing a positively weighted sum of the error or figure of merit (FOM), i.e.,

$$\mathrm{FOM}^2 = \frac{1}{N^2}\sum_{i=1}^{N} w_i[X_i - P_i]^2. \tag{16}$$

For the purposes of calibrating a radiobiological model, X_i is a measurement of some biological end point (e.g. the cell surviving fraction) for the ith experiment, P_i is the model-predicted value for the same end point and experimental conditions, and w_i is the relative weight given to the data for the ith experiment. The experiment weights are normalized such that $\Sigma_i w_i = 1$. The right-hand side of Eq. (16) is divided by the square of the number of data points N so that the FOM gives an indication of the overall quality of a model calibration regardless of the number of data points used to compute the figure of merit.

Data reported in the literature are too often available only in the form of summary figures, and information to estimate the experiment weights, w_i, may not always be available. When the standard error in the measured data is not available, the same value should be used for the experiment weights, i.e., $w_i \propto 1/N$. On the other hand, it is commonly assumed that measurement errors are independent and are distributed normally. In this case, the experiment weights are proportional to the inverse of the variance. Although information on the experiment weights is very desirable, model inputs can still be tuned without this information by giving all or some of the data points the same (or a nominal) value.

A variety of optimization techniques have been developed to locate a parameter set that minimizes the value of a function that depends on one or more independent variables [e.g., see ref. (*46*)]. In the current version of the KBEM software, parameters for the LPL and TLK models (or the RMR model) are tuned using a quasi-Newton gradient technique with an active set strategy (*47–50*), as implemented in Visual Numeric's IMSL® DBCONF routine. Although the FOM can potentially include information from different kinds of experiments (e.g., cell killing and number of DSBs Gy^{-1} $cell^{-1}$), the FOM used in this work includes only data on cell killing as a function of dose and dose rate. The LPL and TLK model parameters are adjusted to minimize the difference between model-predicted and measured estimates of $\bar{L}_f = -\ln S(D)$.

RESULTS[5]

The performance of the TLK and LPL models was tested using a two-step procedure. First, the single-dose and split-dose survival data reported by Stackhouse and Bedford (*25*) were used to generate a model calibration. The survival data include one-fraction exposures delivered at dose rates of 0.12 Gy h^{-1}, 0.5 Gy h^{-1} and 45 Gy h^{-1} as well as survival data for several two-fraction (split-dose) exposures (16 Gy divided into two 8-Gy fractions separated by 1 to 12 h). After a calibration had been generated, the predictive

[4] DSBs Gy^{-1} $cell^{-1}$ estimate is based on a DNA content of approximately 4.682×10^9 bp (*45*).

[5] An executable version of the VC/KBEM application used to perform the reported studies is available by contacting the author at trebor@pnl.gov. See also http://www.pnl.gov/berc/KBEM/VC.

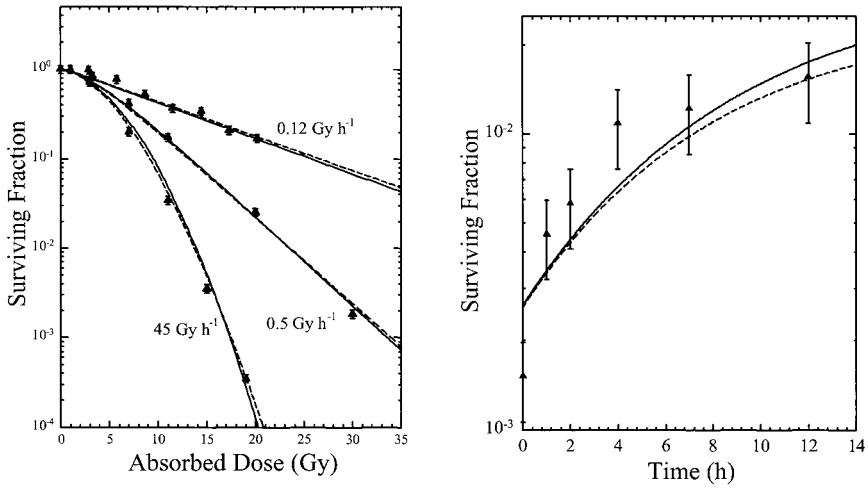

FIG. 1. Survival of plateau-phase CHO 10B2 cells irradiated with ^{137}Cs γ rays. Solid lines, three-parameter LPL model fit ($2Y\Sigma_{dsb}$ = 25 cell^{-1} Gy^{-1}). Dashed lines, four-parameter LPL model fit ($2Y\Sigma_{dsb}$ = 1.77 cell^{-1} Gy^{-1}). Left panel: Cell survival after a single dose of radiation; measured data (*25*) are shown with an estimated standard error of 10% (J. S. Bedford, personal communication). Right panel: Cell survival after split-dose irradiation (8 Gy + 8 Gy); measured data (*25*) are shown with an estimated standard error of 30% (J. S. Bedford, personal communication).

power of the models was tested by comparing measured (*26*) and model-calculated values for the FAR as a function of time after an acute 20-Gy dose of radiation. Model estimates of the initial number of DSBs Gy^{-1} cell^{-1} were also compared to the measured data (*27*). The goodness of fit to the survival data (i.e. the FOM) was used mainly to judge the accuracy of the model calibration. A large value for the FOM could indicate that the model calibration is not reliable or that the postulated mechanisms of action are incomplete or inaccurate. To test the performance of the model more thoroughly, several different sets of parameter constraints were used to generate LPL and TLK model calibrations. The parameter constraints reflect uncertainties associated with the measured data for the initial number of DSBs Gy^{-1} cell^{-1} and the rate of DSB rejoining.

Results with the LPL Model

As a first attempt at model calibration, all four of the LPL model inputs were adjusted to minimize the FOM, subject to the constraints: $0 \le 2Y\Sigma_f \le 1$ cell^{-1} Gy^{-1}, $0 \le 2Y\Sigma_{dsb} \le 40$ cell^{-1} Gy^{-1}, 0.0462 h^{-1} $\le \lambda_{dsb} \le$ 8.32 h^{-1} (equivalent to a 15-h and 5-min DSB repair half-time, respectively), and $0 \le \eta_{dsb} \le 1$ h^{-1}. To maximize the chance that the optimization algorithm would find the best possible model calibration (i.e., the global optimum parameter set), the model optimization was performed several times using different parameter constraints and initial parameter estimates. For all initial parameter sets and constraints investigated, the optimization routine converged to the same optimal parameter set. This observation strongly suggests that a globally optimal calibration was found rather than a locally optimal parameter set. The globally optimal parameter set (rounded to three significant digits) was found to be $2Y\Sigma_f = 3.61 \times 10^{-2}$ fatal lesions cell^{-1} Gy^{-1}, $2Y\Sigma_{dsb} =$ 1.77 Gy^{-1} cell^{-1}, $\lambda_{dsb} = 0.122$ h^{-1} (5.68-h DSB repair half-time), and $\eta_{dsb} = 2.19 \times 10^{-3}$ h^{-1}. The FOM for this parameter set is 4.04%. Because 1.77 DSBs Gy^{-1} cell^{-1} is a factor of 14 lower than the 25 DSBs Gy^{-1} cell^{-1} expected for a CHO cell, this model calibration resulted in a prediction that was clearly inconsistent with independent measurements of the same end point.

As a second attempt at model calibration, $2Y\Sigma_{dsb}$ was set to a value of 25 DSBs Gy^{-1} cell^{-1}, and the other three LPL model inputs were adjusted to minimize the FOM, subject to the constraints: $0 \le 2Y\Sigma_f \le 1$ cell^{-1} Gy^{-1}, 0.0462 h^{-1} $\le \lambda_{dsb} \le$ 8.32 h^{-1} (equivalent to a 15-h and 5-min DSB repair half-time, respectively), and $0 \le \eta_{dsb} \le 1$ h^{-1}. For several different parameter constraints and initial parameter estimates, the optimization routine converged to the same parameter set, which indicates that a globally optimal calibration was found rather than a locally optimal parameter set. The globally optimal parameter set was found to be $2Y\Sigma_f = 4.69 \times 10^{-2}$ fatal lesions cell^{-1} Gy^{-1}, $\lambda_{dsb} = 0.113$ h^{-1} (6.16-h DSB repair half-time), and $\eta_{dsb} = 7.53 \times 10^{-6}$ h^{-1}. The FOM for this parameter set was 4.26%.

Figure 1 shows a comparison of measured and LPL-calculated surviving fractions. The LPL-predicted surviving fraction is in excellent agreement with the measured data for all of the single-dose exposure conditions. For illustrative purposes, the four-parameter fit to the survival data is also shown in Fig. 1. The LPL-predicted trends in the split-dose data show possibly significant deviations from the measured data. For both of the three- and four-parameter calibrations, the LPL model predicts that the split-dose surviving fraction continues to increase for doses separated in time by as much as 10 to 12 h. On the other hand, the measured data for the split-dose exposure conditions suggest that the surviving fraction may reach a maximum for

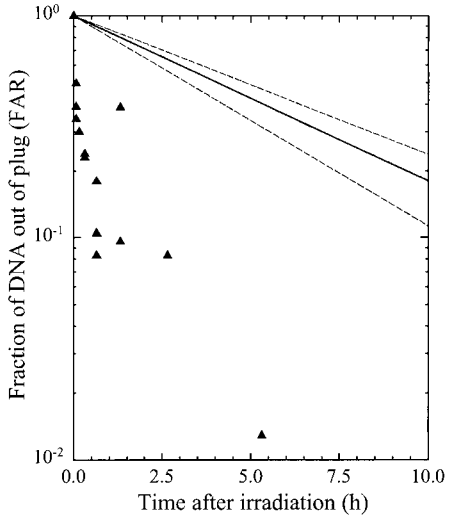

FIG. 2. DSB rejoining kinetics in plateau-phase CHO 10B2 cells after irradiation with 20 Gy delivered at a dose rate of 356.1 Gy h^{-1}. Filled triangles: measured data (*26*). Solid line: three-parameter LPL model fit ($2Y\Sigma_{dsb}$ = 25 $cell^{-1}$ Gy^{-1}). Dashed lines: estimated lower and upper bounds on LPL model rejoining kinetics. Estimated bounds on the FAR are based on (K = 2 Mbp, M_0 = 4,682 × 10^6 bp) and (K = 8 Mbp, M_0 = 50.9 × 10^6 bp). Data for the FAR are normalized to unity 0 h after irradiation.

doses separated by times of the order of 4 to 8 h. Figure 2 shows a comparison of the measured and LPL-predicted rate of DSB rejoining for the three-parameter LPL model calibration. The LPL-predicted data for the rate of DSB rejoining are inconsistent with independent measurements made with a PFGE assay. Moreover, the disagreement between the measured and model-predicted data cannot be easily attributed to uncertainties associated with the gel exclusion parameter or the average chromosome size [refer to Eq. (7)].

A third model calibration was generated using the equality constraints $2Y\Sigma_{dsb}$ = 25 DSBs Gy^{-1} $cell^{-1}$ and λ_{dsb} = 0.231 h^{-1} (3-h DSB repair half-time). The linear repair term was set to correspond to a 3-h repair half-time in an attempt to force the LPL-predicted DSB rejoining kinetics into better agreement with the measured data. The other two LPL model inputs were constrained to $0 \le 2Y\Sigma_f \le 1$ $cell^{-1}$ Gy^{-1} and $0 \le \eta_{dsb} \le 1$ h^{-1}. For this calibration, the binary misrepair term in Eq. (2) was multiplied by a factor of 1/4 as suggested by Sachs *et al.* (*11*). The globally optimal parameter set for this set of parameter constraints was found to be $2Y\Sigma_f$ = 9.20 × 10^{-2} fatal lesions $cell^{-1}$ Gy^{-1} and η_{dsb} = 5.96 × 10^{-5} h^{-1}, and the FOM was 6.57%. Figure 3 shows a comparison of the measured and model-predicted survival data for this calibration. Figure 4 compares the measured and model-predicted rate of DSB rejoining. As the model-predicted DSB rejoining kinetics are forced into better agreement with the measured data (i.e., as the value of λ_{dsb} increases), the goodness of fit to the survival data decreases. These same inconsistencies in LPL model predictions are seen for values of $2Y\Sigma_{dsb}$ in the range from 20 to 40 DSBs Gy^{-1} $cell^{-1}$ (data not shown).

Results with the Two-Lesion Model

Even with a data set as large as the one of Stackhouse and Bedford (*25, 26*), calibration of the eight-parameter TLK model is challenging. If more than six parameters are treated as adjustable, several combinations of model inputs give equally good fits to the survival data. That is, several different parameter sets in the feasible space defined by Eqs. (9), (10) and (11) yield about the same value for the FOM. An effective way to overcome this difficulty is to require that the quantity $2Y(\Sigma_1 + \Sigma_2)$ equal a predetermined value in the range from 20 to 60 DSBs Gy^{-1} $cell^{-1}$ and γ

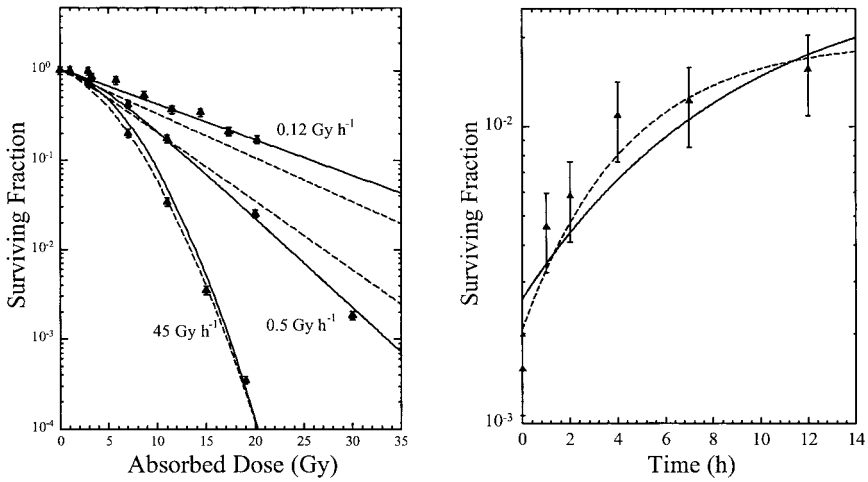

FIG. 3. Survival of plateau-phase CHO 10B2 cells irradiated with ^{137}Cs γ rays. Solid line: three-parameter LPL model fit ($2Y\Sigma_{dsb}$ = 25 $cell^{-1}$ Gy^{-1}). Dashed line: two-parameter LPL model fit [$2Y\Sigma_{dsb}$ = 25 $cell^{-1}$ Gy^{-1}, λ_{dsb} = 0.231 h^{-1} (3-h DSB repair half-time)]. Left panel: cell survival after a single dose of radiation; measured data (*25*) are shown with an estimated standard error of 10% (J. S. Bedford, personal communication). Right panel: cell survival after split-dose irradiation (8 Gy + 8 Gy); measured data (*25*) are shown with an estimated standard error of 30% (J. S. Bedford, personal communication).

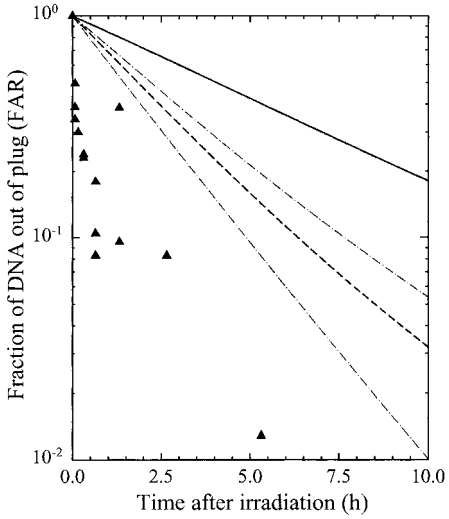

FIG. 4. DSB rejoining kinetics in plateau-phase CHO 10B2 cells after irradiation with 20 Gy delivered at a dose rate of 356.1 Gy h^{-1}. Filled triangles: measured data (*26*). Solid line: three-parameter LPL model fit ($2Y\Sigma_{dsb}$ = 25 $cell^{-1}$ Gy^{-1}). Dashed line: two-parameter LPL model fit [$2Y\Sigma_{dsb}$ = 25 $cell^{-1}$ Gy^{-1}, λ_{dsb} = 0.231 h^{-1} (3-h DSB repair half-time)]. Dash-dot lines: estimated lower and upper bounds on LPL model rejoining kinetics. Estimated bounds on the FAR are based on (K = 2 Mbp, $M_0 = 4{,}682 \times 10^6$ bp) and (K = 8 Mbp, $M_0 = 50.9 \times 10^6$ bp). Data for the FAR are normalized to unity 0 h after irradiation.

= 1/4 as suggested by Sachs *et al.* (*11*). A practical way to implement the $2Y(\Sigma_1 + \Sigma_2)$ constraint is to set $2Y\Sigma_1$ to a specific value (e.g. 20 DSBs Gy^{-1} $cell^{-1}$) and then adjust (optimize) the value of $2Y\Sigma_2$ subject to the constraint that $0 \le 2Y\Sigma_2 \le 40$ DSBs Gy^{-1} $cell^{-1}$. Studies of sensitivity suggest that calibration of the TLK model is not especially sensitive to the *a priori* selection of a value for $2Y\Sigma_1$ for yields in the range from 20 to 30 DSBs Gy^{-1} $cell^{-1}$.

With the constraints γ = 1/4, $2Y\Sigma_1$ = 20 DSBs Gy^{-1} $cell^{-1}$, $0 \le \Sigma_2 \le 40$ DSBs Gy^{-1} $cell^{-1}$, $0 \le a_1, a_2 \le 1$, 2.78×10^{-2} $h^{-1} \le \lambda_1, \lambda_2 \le 8.32$ h^{-1}, and $0 \le \eta \le 1$ h^{-1}, the optimal model calibration was found to be $\lambda_1 = 0.671$ h^{-1} (1.03 h repair half-time), $\beta_1 = 1.52 \times 10^{-3}$, $\Sigma_2 = 5.09$ DSBs Gy^{-1} $cell^{-1}$, $\lambda_2 = 4.39 \times 10^{-2}$ h^{-1} (15.8-h repair half-time), $\beta_2 = 0.00$, and $\eta = 1.18 \times 10^{-4}$ h^{-1}. The FOM for this parameter set was 2.9%. The overall goodness of fit to the survival data is about the same if $2Y\Sigma_1$ is set to a value of 25 or 30 DSBs Gy^{-1} $cell^{-1}$ instead of 20 DSBs Gy^{-1} $cell^{-1}$. For values of $2Y\Sigma_1$ higher than 30 DSBs Gy^{-1} $cell^{-1}$, the FOM tends to increase slightly. As the data shown in Fig. 5 demonstrate, the TLK model does an excellent job of explaining all the single-dose and split-dose survival data. Moreover, a DSB yield of 25.1 Gy^{-1} $cell^{-1}$ (0.536 DSB Gy^{-1} per 100 Mbp) is within the range measured by Cedervall *et al.* (*27*) for CHO cells (0.5 to 0.6 DSB Gy^{-1} per 100 Mbp). On the other hand, the DSB rejoining kinetics predicted with this calibration are not in close agreement with the measured data (Fig. 6).

To improve the agreement with the measured DSB rejoining data, a second model calibration was generated by

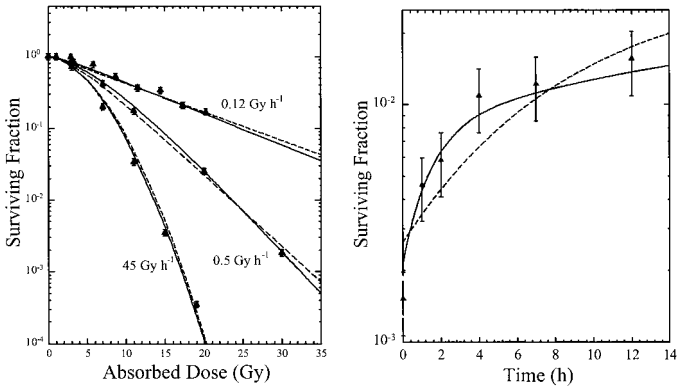

FIG. 5. Survival of plateau-phase CHO 10B2 cells irradiated with ^{137}Cs γ rays. Solid lines: six-parameter TLK model fit (see main text). Dashed lines: three-parameter LPL model fit ($2Y\Sigma_{dsb}$ = 25 $cell^{-1}$ Gy^{-1}). Left panel: cell survival after a single dose of radiation; measured data (*25*) are shown with an estimated standard error of 10% (J. S. Bedford, personal communication). Right panel: cell survival after split-dose irradiation (8 Gy + 8 Gy); measured data (*25*) are shown with an estimated standard error of 30% (J. S. Bedford, personal communication).

setting $\lambda_1 = 2.77$ h^{-1} (15-min repair half-time) and Σ_1 = 20 DSB Gy^{-1} $cell^{-1}$. For this set of equality constraints, the optimal model calibration was found to be $\beta_1 = 0.00$, $\Sigma_2 = 4.43$ DSBs Gy^{-1} $cell^{-1}$, $\lambda_2 = 6.16 \times 10^{-2}$ h^{-1} (11.3 h repair half-time), $\beta_2 = 5.51 \times 10^{-3}$, and $\eta = 4.20 \times 10^{-4}$ h^{-1}. The FOM for this parameter set is 3.3% (compared to 2.9% for the six-parameter calibration). The five-parameter TLK calibration gives excellent agreement with the single-dose survival data (Fig. 7, left panel) and good agreement with the DSB rejoining data (Fig. 8). However, the measured and TLK-predicted surviving fractions for the split-

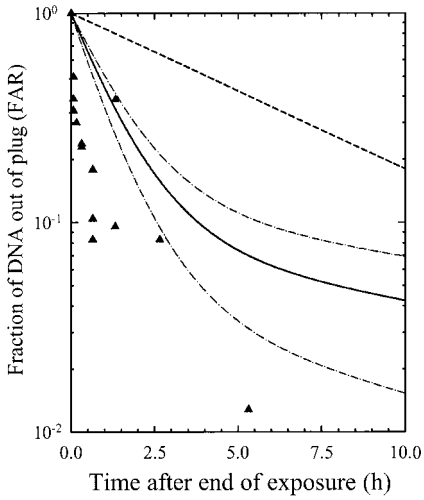

FIG. 6. DSB rejoining kinetics in plateau-phase CHO 10B2 cells after irradiation with 20 Gy delivered at 356.1 Gy h^{-1}. Filled triangles: measured data (*26*). Solid line: six-parameter TLK model (see main text). Dashed line: three-parameter LPL model fit ($2Y\Sigma_{dsb}$ = 25 $cell^{-1}$ Gy^{-1}). Dash-dot lines: estimated lower and upper bounds on TLK model rejoining kinetics. Estimated bounds on the FAR are based on (K = 2 Mbp, $M_0 = 4{,}682 \times 10^6$ bp) and (K = 8 Mbp, $M_0 = 50.9 \times 10^6$ bp). Data for the FAR are normalized to unity 0 h after irradiation.

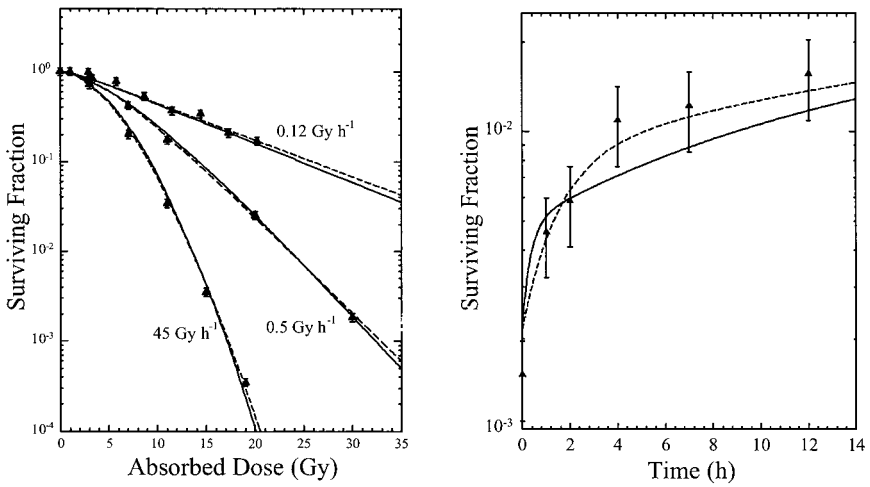

FIG. 7. Survival of plateau-phase CHO 10B2 cells irradiated with ^{137}Cs γ rays. Solid lines: five-parameter TLK model calibration (see main text). Dashed lines: six-parameter TLK model fit (see main text). Left panel: cell survival after a single dose of radiation; measured data (*25*) are shown with an estimated standard error of 10% (J. S. Bedford, personal communication). Right panel: cell survival after split-dose irradiation (8 Gy + 8 Gy); measured data (*25*) are shown with an estimated standard error of 30% (J. S. Bedford, personal communication).

dose exposures (Fig. 7, right panel) show some small inconsistencies, although it is difficult to judge how significant these differences are because of the uncertainties in the measured data. Other TLK model calibrations with λ_1 in the range from 2.77 h^{-1} to 20.79 h^{-1} yield similar results. Larger values of λ_1 (slower repair half-times) tend to improve the fit to the survival data but decrease the agreement with the DSB rejoining data.

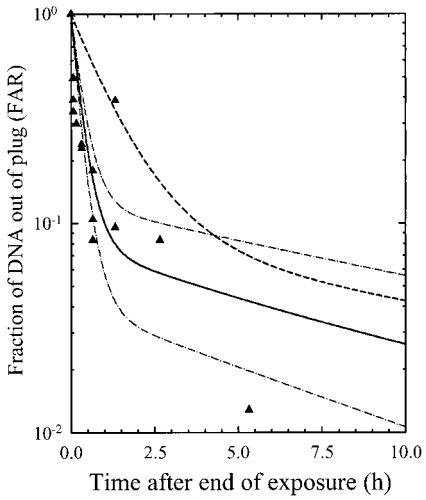

FIG. 8. DSB rejoining kinetics in plateau-phase CHO 10B2 cells after irradiation with 20 Gy delivered at a dose rate of 356.1 Gy h^{-1}. Filled triangles: measured data (26). Solid line: five-parameter TLK model calibration (see main text). Dashed line: six-parameter TLK model calibration (same as Fig. 6). Dash-dot lines: estimated lower and upper bounds on TLK model rejoining kinetics (five-parameter calibration). Estimated bounds on the FAR are based on (K = 2 Mbp, M_0 = 4,682 × 10^6 bp) and (K = 8 Mbp, $M_0 0$ = 50.9 × 10^6 bp). Data for the FAR are normalized to unity 0 h after irradiation.

DISCUSSION

The results shown in Fig. 1 confirm that the LPL model captures the essential trends in the survival data. On the other hand, the LPL model does not provide an entirely satisfactory formalism to establish the putative link between the DSB and cell killing. An initial yield of 1.77 DSBs Gy^{-1} $cell^{-1}$ gives the best agreement with the CHO cell survival data. Similar yields of potentially lethal damage (i.e. $2Y\Sigma_{dsb}$) have been suggested for other mammalian cells (*5*). However, 1.77 DSBs Gy^{-1} $cell^{-1}$ is clearly much lower than the 25 DSBs Gy^{-1} $cell^{-1}$ expected for a CHO cell. When the LPL model is calibrated using the equality constraint 25 DSBs Gy^{-1} $cell^{-1}$, the goodness of fit to the survival data decreases slightly but may still be considered acceptable (see Fig. 1). However, the LPL-predicted DSB rejoining rate for this calibration is not at all consistent with the measured data (Fig. 2).

The parameters of the LPL model can be selected to force the DSB rejoining rate into better agreement with the measured data (Fig 4), but the overall agreement with the cell survival data decreases as the LPL-predicted rate of DSB rejoining increases (Fig. 3). Collectively, these studies strongly suggest that the LPL model does not provide a fully satisfactory formalism to link biochemical processing of the DSB to cell killing. Others have also noted conceptual problems with some aspects of the original LPL model (*8*). The major consequence of the observed discrepancies is that data from PFGE or other DSB assays cannot be used to estimate LPL model inputs reliably.

One way to resolve the apparent inconsistencies among the measured and LPL-predicted data on cell survival and DSB rejoining is to postulate the existence of two distinct kinds of DSBs. Biochemical processing of the two kinds

of DSBs is different because of the local complexity of the damage site. For example, DSBs that contain additional strand breaks or base damage within the same section of the DNA are repaired less efficiently than simple DSBs (two strand breaks on opposite sides of the DNA double helix within about 10 bp). The formalism of the TLK model explicitly considers the possibility that radiation may create two kinds of DSBs. A unique feature of the TLK model is that both kinds of DSBs are allowed to interact in pairwise fashion. Thus DSB repair processes are characterized by two first-order and two second-order repair processes. Double-strand break repair is a first-order process if break ends associated with the same DSBs are rejoined and a second-order process if the break ends associated with two different DSBs are involved in the repair event. Second-order, pairwise damage interaction processes are a central feature of breakage-and-reunion models of chromosome aberration formation (*51, 52*).

Calibration and parameter sensitivity studies suggest that a single set of TLK model inputs can be used to explain experimental observations on the initial number of DSBs Gy^{-1} $cell^{-1}$, the rate of DSB rejoining (Fig. 8), and the data for survival of CHO cells after single-dose and split-dose irradiation (Fig. 7). However, the TLK model calibration that gives the best agreement with the measured data on DSB rejoining (Fig. 8, solid lines) results in some small differences in the data on split-dose survival (Fig. 7, solid lines). These small discrepancies may indicate that additional effects not considered in the present work contribute to biochemical processing of DSBs and cell killing. The data shown in Fig. 5 suggest that the TLK model captures the trends in the survival data better than the LPL model. This observation suggests that both the fast- and slowly rejoining DSBs contribute to cell killing. If only the fast- or slowly rejoining DSBs were responsible for the cell killing effects observed, the LPL model could explain the CHO cell survival data as well as the TLK model.

Studies with the TLK model suggest that both kinds of DSBs make a substantial contribution to the killing of CHO cells by radiation. For an acute 1 Gy dose, the fast-rejoining (simple) DSBs account for approximately 74% of the predicted cell killing effects. At 10 Gy, the fast-rejoining DSBs account for approximately 68% of the lethal DNA damage. These data suggest that the contribution of the slowly rejoining DSBs to cell killing tends to increase as the dose increases. However, this trend and the relative contribution to cell killing of the fast- and slowly rejoining DSBs most likely vary from cell type to cell type. For example, Lange *et al.* (*8*) found that fast- and slowly joining DSBs contributed equally to killing of V79 cells.

Stackhouse and Bedford (*25*) used delayed plating times ranging from 6 to 12 h. Rather than assume *a priori* that all unrepaired DSBs at the time of plating become irreversible and lethal, the model calibrations reported in this work are based on the asymptotic case when an effectively infinite amount of time is available for repair before plating. Because both the LPL and TLK models predict that not all of the initial DSBs are repaired or misrepaired 10 h after irradiation (e.g., see Figs. 6 and 8), the time to plating may have had some impact on the CHO cell survival data. However, the split-dose survival data (Fig. 7, right panel) appear to be close to a plateau after 6 to 8 h. This observation suggests that the majority of the lethal DNA damage was formed during the interval before the cells were plated; i.e., the time available for repair is effectively infinite for plating times greater than 6 to 8 h.

Studies using fixed values for the available repair time also confirm that the time to plating had a minimal effect on the CHO cell survival data. For example, if the TLK model is calibrated using an effective repair time of 10 h, the optimal model calibration is $\lambda_1 = 0.644$ h^{-1} (1.08-h repair half-time), $\beta_1 = 1.71 \times 10^{-3}$, $\Sigma_2 = 6.33$ DSBs Gy^{-1} $cell^{-1}$, $\lambda_2 = 5.65 \times 10^{-2}$ h^{-1} (12.3-h repair half-time), $\beta_2 = 0.00$, and $\eta = 1.09 \times 10^{-4}$ h^{-1}. For an effectively infinite amount of time before plating, the optimal TLK model calibration is $\lambda_1 = 0.671$ h^{-1} (1.03-h repair half-time), $\beta_1 = 1.52 \times 10^{-3}$, $\Sigma_2 = 5.09$ DSBs Gy^{-1} $cell^{-1}$, $\lambda_2 = 4.39 \times 10^{-2}$ h^{-1} (15.8-h repair half-time), $\beta_2 = 0.00$, and $\eta = 1.18 \times 10^{-4}$ h^{-1}. The initial DSB yield increases from 5.09 to 6.33 DSBs Gy^{-1} $cell^{-1}$ and the DSB repair half-time decreases from 15.8 h to 12.3 h. The goodness of fit to the survival data is the same for both parameter sets (i.e., the FOM is 2.9%). The differences between these two model calibrations are not sufficient to resolve the observed inconsistencies in the predicted DSB rejoining data (Fig. 6, solid lines). Other time-to-plating sensitivity studies (not shown) indicate that the trends seen in other LPL and TLK model calibrations are not significantly different for effective repair times in the range from 8 to 12 h.

The TLK model has been developed without specific assumptions about the biochemical mechanisms responsible for the postulated first- and second-order repair processes. Break-end rejoining scenarios can be envisioned in which both the nonhomologous end joining (NHEJ) and the homologous recombination (HR) pathways (*53, 54*) contribute to first- and second-order DSB repair processes. When only a few DSBs are present in a cell, both the NHEJ and HR pathways rejoin DSBs mainly through first-order repair processes, because opportunities for pairwise damage interaction are small. When a large number of DSBs are present in a cell (i.e. at higher doses), two DSBs may be formed in spatial proximity on the same or a different chromosome, and second-order repair processes become more likely. For an acute 1-Gy dose, studies with the TLK model (best-fit calibration) suggest that pairwise damage interaction processes account for about 40% of the lethal DNA damage. At 10 Gy, the proportion of lethal damage formed through binary misrepair increases to 86%. For lower doses, first-order repair events predominate. However, the relative importance of second-order repair processes increases rapidly with dose. The longer a DSB remains in a cell, the higher the probability that the DSB will interact in pairwise fash-

ion. Thus second-order repair processes are more important for the slowly rejoining DSBs than they are for the fast-rejoining DSBs.

If two DSBs in spatial proximity to each other happen to occur in regions of the DNA with sequence homologies (e.g., in the repetitive DNA sequences common to mammalian cells), break ends associated with two different DSBs could be misjoined by HR. The NHEJ pathway can rejoin break ends in regions of the DNA that have few or no sequence homologies (*54*). The specific biochemical pathway that is responsible for the rejoining of a particular break-end pair will most likely depend on factors such as the spatial arrangement of the chromosomes in the nucleus, the state of the chromatin (e.g., binding of the DNA to histone proteins may hold break ends together and facilitate repair), the presence or absence of sequence homologies in a nearby section of undamaged DNA, and the complexity of the damage (e.g., the additional base damage or strand breaks that define a DSB as ''complex'' could hamper HR, NHEJ or both).

In contrast to the current work, Cucinotta *et al.* (*24*) used multistep HR models to link the kinetics of DSB rejoining to the formation of simple exchange-type aberrations. Although they considered only first-order repair events, multistep biochemical repair models can give rise to DSB rejoining kinetics that appears nonexponential or multiexponential because of saturation effects and pathway interactions. Saturation of biochemical repair mechanisms may be important only for high-dose exposure conditions (i.e., under conditions when the number of unrepaired DSBs is much greater than the number of available repair enzymes). On the other hand, pairwise damage interaction processes are determined mainly by spatial and temporal factors that are independent of the biochemical mechanisms of repair. Pairwise damage interaction processes can occur even for very low doses of radiation, because a single ionizing particle is all that is required to create two DSBs in spatial proximity (*33–35*).

To understand the role and relative importance of the multitude of factors and processes that influence damage repair and cellular responses more fully, datasets that are even more comprehensive than the one used in this work are needed. Additional experiments that characterize DSB rejoining kinetics and cell killing as a function of particle LET would be especially useful. High-LET radiation produces pairs of spatially correlated damages more frequently than low-LET radiation (*33–35*), and the binary misrepair interaction probability η (or η_1, η_2 and $\eta_{1,2}$) should increase as the particle LET increases (a proximity effect). Also, experimental and theoretical studies (*55, 56*) suggest that the ratio of complex to simple damages (i.e., the ratio of Σ_2 to Σ_1) most likely increases as particle LET increases. On the other hand, the repair characteristics of the individual damage types (λ_1, λ_2, a_1, a_2, β_1 and β_2) and the damage fixation probabilities ε_1 and ε_2 are most likely independent, or almost independent, of particle LET.

For routine applications, calibration of the TLK model will most likely be limited to adjusting a few key parameters. Parameter sensitivity studies suggest that an effective strategy is to use the available cell survival data to tune the η, λ_1 and λ_2 DSB rejoining parameters and the damage yield parameter Σ_2. Other model inputs can be set *a priori* to reasonable values such as $\Sigma_1 = 20$ DSBs Gy^{-1} cell^{-1}, $a_1 = a_2 = 0$, $\beta_1 = 0.00$, $\beta_2 = 5 \times 10^{-3}$, and $\gamma = 0.25$. Calibration of the TLK model is not overly sensitive to the *a priori* selection of a particular value for the quantity $2Y(\Sigma_1 + \Sigma_2)$. For CHO cells, values of $2Y(\Sigma_1 + \Sigma_2)$ in the range from about 20 to 30 DSBs Gy^{-1} cell^{-1} appear optimal.

Although calibrating the TLK model using cell survival data will yield better results for applications such as radiation therapy where tumor cell killing is to be maximized, some model inputs can most likely be adjusted directly or indirectly to reflect data from assays for DNA damage or chromosome damage. For example, data from PFGE assays could be used to scale the DSB yield $2Y(\Sigma_1 + \Sigma_2)$ to better reflect the characteristics of a particular cell line. Alternatively, the fast-rejoining rate parameter λ_1 could be set to a value that is consistent with experimental observations on the initial DSB rejoining rate. It may also be possible to estimate Σ_1 and Σ_2 directly using *ab initio* (Monte Carlo) damage formation models. Nikjoo *et al.* (*55*) estimate that about 30% of the DSBs produced by low-LET radiation are accompanied by additional strand breaks and may be considered ''complex''. For comparison, the studies reported here suggest that approximately 20% of the initial DSBs are complex, as judged by their damage rejoining kinetics. If the reasonable agreement between these values is not purely fortuitous, the LET dependence of Σ_1 and Σ_2 can most likely be predicted from first principles.

CONCLUSIONS

The studies reported here demonstrate that the TLK model provides a more satisfactory formalism to link biochemical processing of the DSB to cell killing than the LPL model. A single set of TLK model inputs gives reasonable agreement with all the measured cell survival data, the initial yield of DSBs Gy^{-1} cell^{-1}, and the rate of DSB rejoining. The reported studies support the hypothesis that radiation creates fast- and slowly repairing DSBs. About 20 DSBs Gy^{-1} cell^{-1} are rejoined quickly (15-min repair half-time), and 4 to 6 DSBs Gy^{-1} cell^{-1} are rejoined very slowly (10 to 15-h repair half-time). Split-dose experiments with CHO cells by Nelson *et al.* (*57*) also indicate that DNA damage with repair half-times of the order of 18 h may be involved in cell killing. Both kinds of DSBs make a substantial contribution to the killing of CHO cells by radiation.

Sensitivity studies suggest that, even with the two first-order repair processes and two second-order repair processes included in the TLK model, some small differences

are seen among the measured and predicted CHO cell survival and DSB rejoining data. These inconsistencies suggest that effects not considered in the present work may affect biochemical processing of the DSB and hence cell killing. In contrast, Lange *et al.* (*8*) found that two first-order DSB repair processes were sufficient to link biochemical processing of the DSB to cell killing. Large, multi-end point datasets, such as the one of Stackhouse and Bedford (*25, 26*), can provide useful tests of the putative, sometimes subtle processes linking initial radiation damage to higher-level cellular responses. Future work should expand the model testing and intercomparison studies reported here to include other radiobiological models (*7–10, 24*).

ACKNOWLEDGMENTS

The author thanks Dr. J. S. Bedford for providing the measured data in tabular form, R. T. Marler and Dr. J. Malard for direction and discussion on the use of optimization algorithms, J. R. Weber for editorial assistance, and the reviewers for constructive comments and criticism on the original manuscript. This work was supported by the U.S. Department of Energy under contract DE-AC06-76RLO 1830.

Received: February 14, 2001; accepted: June 18, 2001

REFERENCES

1. G. W. Barendsen, Dose fractionation, dose rate and isoeffect relationships for normal tissue responses. *Int. J. Radiat. Oncol. Biol. Phys.* **8**, 1981–1997 (1982).
2. D. J. Brenner, L. R. Hlatky, P. J. Hahnfeldt, Y. Huang and R. K. Sachs, The linear-quadratic model and most other common radiobiological models result in similar predictions of time–dose relationships. *Radiat. Res.* **150**, 83–91 (1998).
3. R. G. Dale, The application of the linear-quadratic dose–effect equation to fractionated and protracted radiotherapy. *Br. J. Radiol.* **58**, 515–528 (1985).
4. P. Nilsson, H. D. Thames and M. C. Joiner, A generalized formulation of the 'incomplete-repair' model for cell survival and tissue response to fractionated low dose-rate irradiation. *Int. J. Radiat. Biol.* **57**, 127–142 (1990).
5. S. B. Curtis, Lethal and potentially lethal lesions induced by radiation—A unified repair model. *Radiat. Res.* **106**, 252–270 (1986); Erratum, *Radiat. Res.* **119**, 584 (1989).
6. C. A. Tobias, The repair-misrepair model in radiobiology: Comparison to other models. *Radiat. Res.* **104** (Suppl.), 77–95 (1985).
7. R. B. Hawkins, A microdosimetric-kinetic model of cell death from exposure to ionizing radiation of any LET, with experimental and clinical applications. *Int. J. Radiat. Biol.* **69**, 739–755 (1996).
8. C. S. Lange, P. J. Mayer and N. M. Reddy, Tests of double-strand break, lethal-potentially lethal and repair-misrepair models for mammalian cell survival using data for survival as a function of delayed-plating interval for log-phase Chinese hamster V79 cells. *Radiat. Res.* **148**, 285–292 (1997).
9. J. Y. Ostashevsky, A model relating cell survival to DNA fragment loss and unrepaired double-strand breaks. *Radiat. Res.* **118**, 437–466 (1989).
10. J. Y. Ostashevsky, Cell recovery kinetics for split-dose, multifractionated and continuous irradiation in the DSB model. *Int. J. Radiat. Biol.* **63**, 47–58 (1993).
11. R. K. Sachs, P. Hahnfeld and D. J. Brenner, The link between low-LET dose-response relations and the underlying kinetics of damage production/repair/misrepair. *Int. J. Radiat. Biol.* **72**, 351–374 (1997).
12. B. Fertil, I. Reydellet and P. J. Deschavanne, A benchmark of cell survival models using survival curves for human cells after completion of repair of potentially lethal damage. *Radiat. Res.* **138**, 61–69 (1994).
13. W. Sontag, Comparison of six different models describing survival of mammalian cells after irradiation. *Radiat. Environ. Biophys.* **29**, 185–201 (1990).
14. J. S. Bedford, Sublethal damage, potentially lethal damage, and chromosomal aberrations in mammalian cells exposed to ionizing radiations. *Int. J. Radiat. Oncol. Biol. Phys.* **21**, 1457–1469 (1991).
15. P. L. Olive, The role of DNA single- and double-strand breaks in cell killing by ionizing radiation. *Radiat. Res.* **150** (Suppl.), S42–S51 (1998).
16. M. Frankenberg-Schwager and D. Frankenberg, DNA double-strand breaks: Their repair and relationship to cell killing in yeast. *Int. J. Radiat. Biol.* **58**, 569–575 (1990).
17. C. Badie, G. Iliakis, N. Foray, G. Alsbeih, B. Cedervall, N. Chavaudra, G. Pantelias, C. Arlett and E. P. Malaise, Induction and rejoining of DNA double-strand breaks and interphase chromosome breaks after exposure to X rays in one normal and two hypersensitive human fibroblast cell lines. *Radiat. Res.* **144**, 26–35 (1995).
18. E. Dikomey, Induction and repair of DNA strand breaks in X-irradiated proliferating and quiescent CHO cells. *Int. J. Radiat. Biol.* **57**, 1169–1182 (1990).
19. J. Dahm-Daphi and E. Dikomey, Rejoining of DNA double-strand breaks in X-irradiated CHO cells studied by constant- and graded-field gel electrophoresis. *Int. J. Radiat. Biol.* **69**, 615–621 (1996).
20. G. Iliakis, D. Blöcher, L. Metzger and G. Pantelias, Comparison of DNA double-strand break rejoining as measured by pulsed field gel electrophoresis, neutral sucrose gradient centrifugation and non-unwinding filter elution in irradiated plateau-phase CHO cells. *Int. J. Radiat. Biol.* **59**, 927–939 (1991).
21. T. Radivoyevitch, D. G. Hoel, P. J. Hahnfeldt, B. Rydberg and R. K. Sachs, Recent data obtained by pulsed-field gel electrophoresis suggest two types of double-strand breaks. *Radiat. Res.* **149**, 52–58 (1998).
22. M. Frankenberg-Schwager, Induction, repair and biological relevance of radiation induced DNA lesions in eukaryotic cells. *Radiat. Environ. Biophys.* **29**, 273–292 (1990).
23. D. T. Goodhead, Saturable repair models of radiation action in mammalian cells. *Radiat. Res.* **104** (Suppl.), S58–S67 (1985).
24. F. A. Cucinotta, H. Nikjoo, P. O'Neill and D. T. Goodhead, Kinetics of DSB rejoining and formation of simple chromosome exchange aberrations. *Int. J. Radiat. Biol.* **76**, 1463–1474 (2000).
25. M. A. Stackhouse and J. S. Bedford, An ionizing radiation-sensitive mutant of CHO cells: irs-20. II. Dose-rate effects and cellular recovery processes. *Radiat. Res.* **136**, 250–254 (1993).
26. M. A. Stackhouse and J. S. Bedford, An ionizing radiation-sensitive mutant of CHO cells: irs-20. III. Chromosome aberrations, DNA breaks and mitotic delay. *Int. J. Radiat. Biol.* **65**, 571–582 (1994).
27. B. Cedervall, R. Wong, N. Albright, J. Dynlacht, P. Lambin and W. C. Dewey, Methods for the quantification of DNA double-strand breaks determined from the distribution of DNA fragment sizes measured by pulsed-field gel electrophoresis. *Radiat. Res.* **143**, 8–16 (1995); Erratum, *Radiat. Res.* **144**, 122 (1995).
28. D. D. Ager, J. W. Phillips, E. A. Columna, R. A. Winegar and W. F. Morgan, Analysis of restriction enzyme-induced DNA double-strand breaks in Chinese hamster ovary cells by pulsed-field gel electrophoresis: Implications for chromosome damage. *Radiat. Res.* **128**, 150–156 (1991).
29. J. L. Schwartz, Alterations in chromosome structure and variations in the inherent radiation sensitivity of human cells. *Radiat. Res.* **149**, 319–324 (1998).
30. J. R. Savage, The transmission of FISH-painted patterns derived from complex chromosome exchanges. *Mutat. Res.* **347**, 87–95 (1995).
31. N. L. Oleinick and S. M. Chiu, Nuclear and chromatin structures and their influence on the radiosensitivity of DNA. *Radiat. Prot. Dosim.* **52**, 353–358 (1994).
32. P. J. Johnston, P. L. Olive and P. E. Bryant, Higher-order chromatin

structure-dependent repair of DNA double-strand breaks: Modeling the elution of DNA from nucleoids. *Radiat. Res.* **148**, 561–567 (1997).

33. H. C. Newman, K. M. Prise and B. D. Michael, The role of higher-order chromatin structure in the yield and distribution of DNA double-strand breaks in cells irradiated with X-rays or alpha-particles. *Int. J. Radiat. Biol.* **76**, 1085–1093 (2000).

34. W. R. Holley and A. Chatterjee, Clusters of DNA damage induced by ionizing radiation: Formation of short DNA fragments. I. Theoretical modeling. *Radiat. Res.* **145**, 188–199 (1996).

35. B. Rydberg, Clusters of DNA damage induced by ionizing radiation: Formation of short DNA fragments. II. Experimental detection. *Radiat. Res.* **145**, 200–209 (1996).

36. W. B. Coleman and G. J. Tsongalis, Multiple mechanisms account for genomic instability and molecular mutation in neoplastic transformation. *Clin. Chem.* **41**, 644–657 (1995).

37. P. C. Hanawalt, Genomic instability: environmental invasion and the enemies within. *Mutat. Res.* **25**, 117–125 (1998).

38. C. Schmutte and R. Fishel, Genomic instability: First step to carcinogenesis. *Anticancer Res.* **19**, 4665–4696 (1999).

39. R. D. Stewart, J. K. Shultis and B. A. Montelone, *A Kinetic Biological Effects Model for Quiescent Cells.* Report PNNL-SA-30807, Pacific Northwest National Laboratory, Richland, WA, 2000. [Available online at http://www.pnl.gov/berc/epub/pnnl30807/]

40. C. W. Gear, Chapter 11 in *Numerical Initial Value Problems in Ordinary Differential Equations.* Prentice-Hall, Englewood Cliffs, NJ, 1971.

41. L. F. Shampine and C. W. Gear, A user's view of solving stiff ordinary differential equations. *SIAM Rev.* **21**, 1–17 (1979).

42. C. R. Contopoulou, V. E. Cook and R. K. Mortimer, Analysis of DNA double strand breakage and repair using orthogonal field alternation gel electrophoresis. *Yeast* **3**, 71–76 (1987).

43. V. E. Cook and R. K. Mortimer, A quantitative model of DNA fragments generated by ionizing radiation, and possible experimental applications. *Radiat. Res.* **125**, 102–106 (1991).

44. M. Belli, R. Cherubini, M. D. Vecchia, V. Dini, G. Moschini, C. Signoretti, G. Simone, M. A. Tabocchini and P. Tiveron, DNA DSB induction and rejoining in V79 cells irradiated with light ions: A constant field gel electrophoresis study. *Int. J. Radiat. Biol.* **76**, 1095–1104 (2000).

45. W. Sontag, G. Knedlitschek, K. F. Weibezahn and H. Dertinger, The DNA content of some mammalian cells measured by flow cytometry and its influence on radiation sensitivity. *Int. J. Radiat. Biol.* **57**, 1183–1193 (1990).

46. W. H. Press, S. A. Teukolsky, W. T. Vetterling and B. P. Flannery, *Numerical Recipes in FORTRAN*: *The Art of Scientific Computing.* 2nd ed. Cambridge University Press, New York, 1992.

47. J. E. Dennis, Jr. and R. B. Schnabel, *Numerical Methods for Unconstrained Optimization and Nonlinear Equations.* Prentice-Hall, Englewood Cliffs, NJ, 1983.

48. P. E. Gill and W. Murray, *Minimization Subject to Bounds on the Variables.* NPL Report NAC 72, National Physical Laboratory, Middlesex, UK, 1976.

49. P. E. Gill, W. Murray and M. Wright, *Practical Optimization.* Academic Press, New York, 1981.

50. P. E. Gill, W. Murray, M. A. Saunders and M. H. Wright, Model building and practical aspects of nonlinear programming. In *Computational Mathematical Programming* (K. Schittkowski, Ed.). NATO ASI Series 15, Springer-Verlag, Berlin, 1985.

51. J. R. Savage, A brief survey of aberration origin theories. *Mutat. Res.* **404**, 139–47 (1998).

52. R. K. Sachs, A. Rogoff, A. M. Chen, P. J. Simpson, J. R. Savage, P. Hahnfeldt and L. R. Hlatky, Underprediction of visibly complex chromosome aberrations by a recombinational-repair ('one-hit') model. *Int. J. Radiat. Biol.* **76**, 129–148 (2000).

53. P. A. Jeggo, Identification of genes involved in repair of DNA double-strand breaks in mammalian cells. *Radiat. Res.* **150** (Suppl.), S80–S91 (1998).

54. L. K. Lewis and M. A. Resnick, Tying up loose ends: Nonhomologous end-joining in *Saccharomyces cerevisiae*. *Mutat. Res.* **451**, 71–89 (2000).

55. H. Nikjoo, P. O'Neill, M. Terrissol and D. T. Goodhead, Quantitative modelling of DNA damage using Monte Carlo track structure method. *Radiat. Environ. Biophys.* **38**, 31–38 (1999).

56. R. Roots, G. Kraft and E. Gosschalk, The formation of radiation-induced DNA breaks: The ratio of double-strand breaks to single-strand breaks. *Int. J. Radiat. Oncol. Biol. Phys.* **11**, 259–265 (1985).

57. J. M. Nelson, L. A. Braby, N. F. Metting and W. C. Roesch, Multiple components of split-dose repair in plateau-phase mammalian cells: A new challenge for phenomenological modelers. *Radiat. Res.* **121**, 154–160 (1990).